

## ADVANCEMENTS IN FUNDAMENTAL FREQUENCY IMPEDANCE BASED EARTH-FAULT LOCATION IN UNEARTHED DISTRIBUTION NETWORKS

Janne ALTONEN

ABB Oy Distribution Automation – Finland  
[janne.altonen@fi.abb.com](mailto:janne.altonen@fi.abb.com)

Ari WAHLROOS

ABB Oy Distribution Automation – Finland  
[ari.wahlroos@fi.abb.com](mailto:ari.wahlroos@fi.abb.com)

### ABSTRACT

Impedance based fault location algorithms utilizing fundamental frequency phasors have become an industry standard in modern microprocessor-based protection relays. Their performance has proven to be satisfactory in locating short-circuit faults, but locating earth faults in unearthed distribution systems has been a challenge until now. This paper studies some of the key factors decreasing the earth-fault location accuracy of the traditional distance relay type of algorithms. The influence of the following parameters is investigated: zero sequence charging current and load of the feeder, fault resistance and fault current magnitude. Computer simulations and field test recordings from a real utility network are used to illustrate the influence. The study is based on two network models with symmetrical components. Finally, a new algorithm is introduced as a solution to the problem described above.

### INTRODUCTION

It is a well-known fact that the most common fault type in electrical distribution networks is a single phase-to-earth fault. According to earlier studies, for instance, in the Nordic countries, about 50-80 % of the faults are of this type [1]. As utilities today focus on continuity, dependability and reliability of their networks, fault location has become an important supplementary function of relay terminals. In the past many attempts have been made and numerous methods have been suggested to find a practically applicable algorithm for earth-fault distance calculation in unearthed distribution systems, e.g. [2], but so far, no such algorithms have been introduced commercially. This paper explains the problems of locating earth faults in unearthed distribution networks by using fundamental frequency phasors, and proposes a new algorithm as a solution to this problem.

### BACKGROUND AND THEORY

The analysis is based on the theory of symmetrical components. Two different network models based on symmetrical components are used in the study:

1. A model, where the fault is located in front of the equivalent load tap.
2. A model, where the fault is located behind the equivalent load tap.

These network models are illustrated in Fig. 1 and 2.

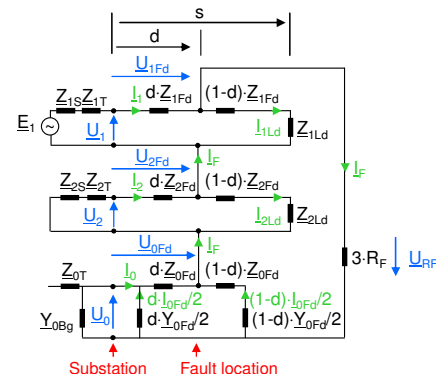


**Figure 1.** Symmetrical component equivalent circuit for a single phase-to-earth fault located in front of the equivalent load tap.

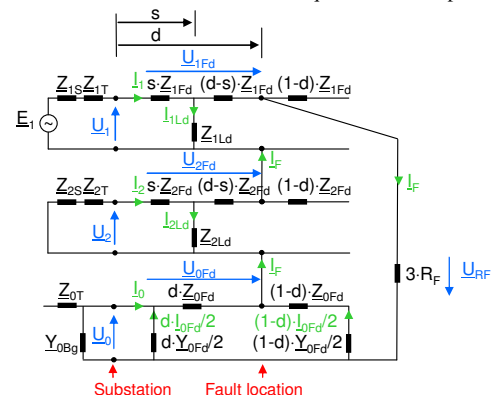


**Figure 2.** Symmetrical component equivalent circuit for a single phase-to-earth fault located behind the equivalent load tap.

The following notations are used in Fig. 1 and 2:

- $d$  = Per unit fault distance ( $d = 0 \dots 1$ ).
- $s$  = Per unit distance of the equivalent load tap ( $s = 0 \dots 1$ ).
- $Z_{1S}$  = Positive sequence source impedance.
- $Z_{1T}$  = Positive sequence impedance of the main transformer.
- $Z_{1Fd}$  = Positive sequence impedance of the protected feeder.
- $Z_{1Ld}$  = Positive sequence impedance of the load.
- $Z_{2S}$  = Negative sequence source impedance.
- $Z_{2T}$  = Negative sequence impedance of the main transformer.
- $Z_{2Fd}$  = Negative sequence impedance of the protected feeder.
- $Z_{2Ld}$  = Negative sequence impedance of the load.
- $Z_{0T}$  = Zero sequence impedance of the main transformer.
- $Z_{0Fd}$  = Zero sequence impedance of the protected feeder.
- $Y_{0Bg}$  = Phase-to-earth admittance of the background network per phase.
- $Y_{0Fd}$  = Phase-to-earth admittance of the protected feeder per phase.
- $R_F$  = Fault resistance.
- $I_1$  = Positive sequence current measured at relay location.
- $I_{1Ld}$  = Positive sequence load current.
- $I_2$  = Negative sequence current measured at relay location.
- $I_{2Ld}$  = Negative sequence load current.
- $I_0$  = Zero sequence current measured at relay location.
- $I_{0Fd}$  = Zero sequence charging current of the feeder.
- $I_F$  = Fault component current at fault location.
- $U_1$  = Positive sequence voltage measured at relay location.
- $U_2$  = Negative sequence voltage measured at relay location.
- $U_0$  = Zero sequence voltage measured at relay location.

The equivalent load tap and its distance introduced in Fig. 2 represents a fictional load tap at a per unit distance  $s$  from the substation. The derivation and meaning of this parameter are illustrated in Fig. 3, where the load is assumed to be evenly distributed along the feeder. The maximum value of the voltage drop, denoted  $U_{drop(real)}$ , appears in the end of the line. Parameter  $s$  is the distance at which a single load tap corresponding to the total load of the feeder would result in a voltage drop equal to  $U_{drop(real)}$ . The dashed curve in Fig. 3 shows the voltage drop profile in this case.

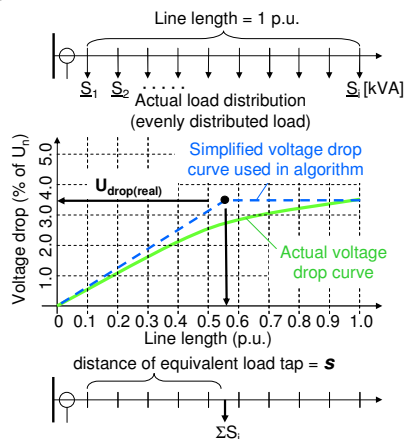


Figure 3. Description of the equivalent load distance.

The value of  $s$  can be estimated based on load flow and voltage drop calculations using Eq. 1:

$$s = U_{drop(real)} / U_{drop(s=1)} \quad (1)$$

where

$U_{drop(real)}$  = the actual maximum voltage drop of the feeder  
 $U_{drop(s=1)}$  = the fictional voltage drop if the entire load would be tapped at the end of the feeder.

Alternatively, parameter  $s$  can be calculated based on the voltages and currents measured by conducting a single-phase earth-fault test ( $R_F = 0$  ohm) at that point of the feeder where the maximum actual voltage drop takes place. The equation for parameter  $s$  can be derived from Fig. 2 by inserting  $d$  equal to the per unit distance corresponding to the actual location of the earth-fault test.

Based on the equivalent circuit diagrams of Fig. 1 and 2, the following equations can be written. If the fault is located in front of the equivalent load tap ( $d \leq s$ ), then Eq. 2 applies (refer to Fig. 1):

$$\begin{aligned} U_0 + U_1 + U_2 &= U_{0Fd} + U_{1Fd} + U_{2Fd} + U_{RF} = \dots \\ d \cdot Z_{1Fd} \cdot I_1 + d \cdot Z_{2Fd} \cdot I_2 + d \cdot Z_{0Fd} \cdot (I_0 + d \cdot I_{0Fd}/2) + 3 \cdot R_F \cdot I_F & \quad (2) \end{aligned}$$

If the fault is located behind the equivalent load tap ( $d \geq s$ ), then Eq. 3 applies (refer to Fig. 2):

$$\begin{aligned} U_0 + U_1 + U_2 &= U_{0Fd} + U_{1Fd} + U_{2Fd} + U_{RF} = \dots \\ s \cdot Z_{1Fd} \cdot I_1 + (d-s) \cdot Z_{1Fd} \cdot I_F + s \cdot Z_{2Fd} \cdot I_2 + (d-s) \cdot Z_{2Fd} \cdot I_F + \dots \\ d \cdot Z_{0Fd} \cdot (I_0 + d \cdot I_{0Fd}/2) + 3 \cdot R_F \cdot I_F & \quad (3) \end{aligned}$$

The voltage and current terms in the equations correspond to the notations used in Fig. 1 and 2 and are selected as follows:  $\underline{U}_1 = \underline{U}_1$ ,  $\underline{U}_2 = \underline{U}_2$ ,  $\underline{U}_0 = \underline{U}_0$ ,  $\underline{I}_1 = \underline{I}_1$ ,  $\underline{I}_2 = \underline{I}_2$ ,  $\underline{I}_0 = \underline{I}_0$ ,  $\underline{I}_F = \underline{I}_F = \underline{I}_0 + \underline{I}_{0Fd}$ ,  $\underline{I}_{0Fd} = \underline{I}_{0Fd}$ , where  $\Delta$  indicates a change from pre-fault to fault conditions.

The key terms in Eq. 2 and 3 are the currents flowing through the fault resistance and the zero sequence impedance of the feeder. Considering the latter current term, it is composed of two parts:

1. One part, which does not depend on the location of the fault, only on the background network ( $\underline{I}_0$ ).
2. A second part, which depends on the location of the fault and on the parameters of the faulted feeder itself ( $d \cdot \underline{I}_{0Fd}$ ).

The term  $d \cdot \underline{I}_{0Fd}$  is neglected in the traditional distance relay type of algorithms, as it cannot be directly measured. This term is dependent on the fault location and on the phase-to-earth admittance of the feeder. It increases linearly, if  $\underline{I}_{0Fd}$  is assumed to be evenly distributed along the feeder. This is illustrated in Fig. 4.

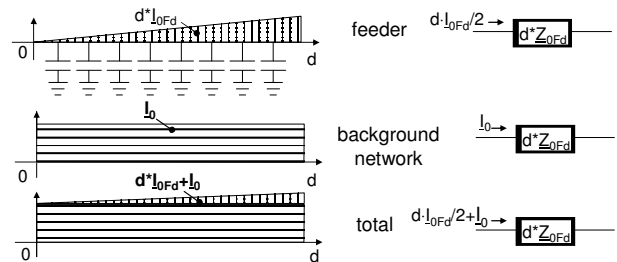


Figure 4. Zero sequence current distribution of the faulted feeder and its modeling.

The approximation used in the modeling is that half of the total zero-sequence charging current from the substation to the fault point flows through the zero sequence impedance and therefore the term  $d \cdot \underline{I}_{0Fd}$  is divided by 2 in Eq. 2 and 3. The magnitude of  $\underline{I}_{0Fd}$  can be calculated from the phase-to-earth capacitance of the feeder or it can be measured when an earth fault occurs on another feeder.

The per unit fault distance  $d$  can be obtained from Eq. 2 and 3 by splitting them into real and imaginary parts. The resulting equation is a second order polynomial. The root, the value of which is between 0...1 is the valid fault distance. The logic for selecting between the results from Eq. 2 and 3 is based on calculated fault distance estimates: if  $d$  of Eq. 2 is less than  $s$ , then this is the valid fault distance estimate, otherwise the distance estimate is taken from Eq. 3.

### EARTH-FAULT SIMULATIONS

The performance of Eq. 2 and 3 is tested with simulated data from the PSCAD/EMTDC transient simulation program. The simulated network represents a rural power system with a 110/20 kV, 50 Hz substation. The faulty

feeder is a radial 20 km long OH-feeder consisting of a Raven conductor (Al/Fe 54/9). Earth faults are placed along the feeder from the substation at steps of 0.1 per unit (0.1, 0.2, ..., 1.0 p.u.).

First the influence of the zero sequence charging current of the feeder is studied in no-load condition. The importance of considering this current term is clearly shown by Fig. 5. If the charging current is excluded, the error is significant, especially with higher fault resistances.

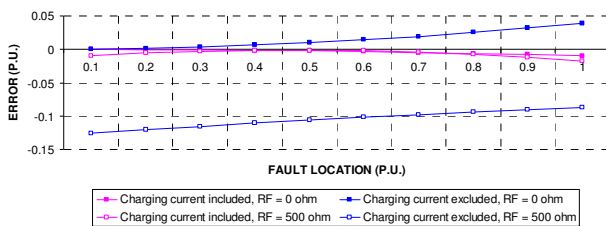


Figure 5. Influence of current term selection in Eq. 2 and 3.

Next, the influence of the load distribution is analyzed. A simulation where 1 MVA load ( $\cos(\varphi) = 0.9$ ) is either tapped at the midpoint or evenly distributed along the 20 km feeder is made. As shown in Fig. 6 both Eq. 2 and Eq. 3 are needed to minimize the errors at distributed load, which is the most realistic assumption in the case of a real distribution feeder.

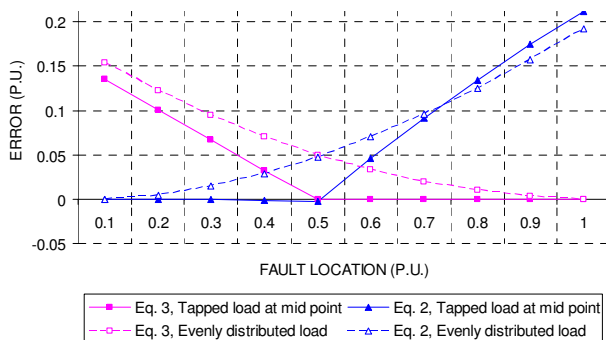


Figure 6. Influence of load distribution in Eq. 2 and 3.

The influence of the fault current (at fault point with  $R_F = 0$  ohm) versus load current magnitude is studied in Fig. 7. The fault current variations are 23 A, 33 A and 62 A, the load current being 29 A. Then the ratio  $I_F/I_{Load}$  is 0.8, 1.1 and 2.1. As shown in Fig. 7, the fault distance estimation error is related to the ratio of magnitudes of the fault current and the load current. According to the simulations made, the fault current should exceed the load current in order to minimize errors in fault location. Especially this applies to Eq.2 ( $d \leq s$ ). Unless met in normal operation, this condition can be achieved by means of some manual or automatic switching operations in the background network e.g. during the dead time of the delayed auto-reclosing sequence.

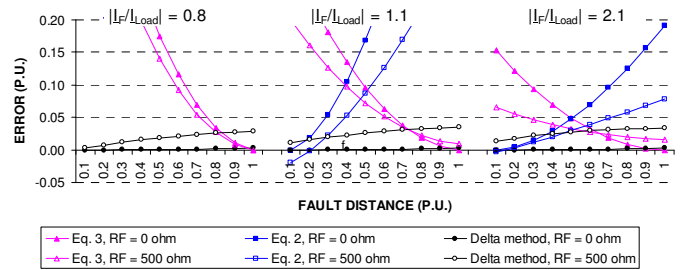


Figure 7. Influence of fault current vs. load current magnitude.

The error related to the fault current and the load current magnitude can be practically eliminated, if Eq. 2 or 3 are used with the pre-change and post-change voltage and current values during the fault itself. This change either reduces or increases the fault current and it may be caused e.g. by an automatic switching operation in the background network during the fault. In this case, the voltage and current terms are preferably selected as follows:  $\underline{U}_1 = \Delta \underline{U}_1$ ,  $\underline{U}_2 = \Delta \underline{U}_2$ ,  $\underline{U}_0 = \Delta \underline{U}_0$ ,  $\underline{I}_1 = \Delta \underline{I}_1$ ,  $\underline{I}_2 = \Delta \underline{I}_2$ ,  $\underline{I}_0 = \Delta \underline{I}_0$ ,  $\underline{I}_{Fsd} = \Delta \underline{I}_{Fsd}$ , where  $\Delta$  indicates a change from pre-change to post-change conditions during the fault. The notations correspond to the notations used in Fig. 1 and 2. In Fig. 7 the simulation result of this method is marked “Delta method”.

Based on the above analysis, the main reasons why the traditional distance relay type of algorithms cannot be used for earth-fault location in unearthed networks are the shortages in the primary circuit modeling that form the basis for the algorithm design: ignorance of the zero sequence charging current and mismatch of the modeled and actual load distribution. Due to these shortages in modeling, the fault current in unearthed distribution networks will be too small to allow a satisfactory fault location accuracy.

### FIELD TESTING AND EXPERIENCE

In recent years, ABB Oy, Distribution Automation, Finland has made intensive field tests in co-operation with some Finnish power utilities in order to test and develop new earth-fault location algorithms and gather data from distribution networks. Since 2004 almost 800 earth-fault tests have been recorded and evaluated. Below, one field test series is studied. These tests were made in the 20 kV, 50 Hz rural distribution network of the utility of Savon Voima Oy, near the city of Nilsia in Finland. The test feeder configuration is illustrated in Fig. 8. A special feature of this 110/20 kV substation is that the 20 kV voltages and currents are measured with sensors, the currents with Rogowski coils and the voltages with resistive dividers. The high linearity and wide dynamics of sensors are optimal, when low-amplitude fault quantities are measured. Thanks to the high linearity of sensors, also phase and amplitude error corrections can be easily implemented in a relay terminal.

**Feeder parameters:**

- $Z_{FD} = (17.1 + j \cdot 10.3) \text{ ohm}$
- $Z_{DFD} = (21.5 + j \cdot 55.1) \text{ ohm}$
- $S = 0.4$
- $3I_{FD} = 5 \text{ A}$
- $3I_{DF} = 30 \dots 40 \text{ A}$
- Total length: 84 km
- Length of the main line: 29 km
- Number of distribution transformers: 81
- Peak load: 1.2 MW

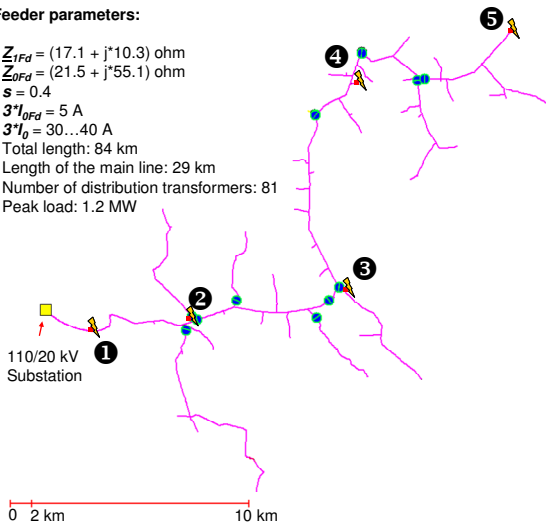


**Figure 8.** Test feeder configuration.

A summary of the test results is shown in Table 1. The results are from five different fault locations with two different fault resistance values, 0 and 500 ohms. The fault resistance is purely resistive and it is composed of ceramic resistor disks assembled on a rod and earthed to the low voltage (LV) side system earthing electrode with an impedance of a few ohms as illustrated in Fig. 9b.

**Table 1.** Field test results.

| Fault location # | Fault dist. (p.u.) | Estimated dist. (p.u.) | Error (p.u.) | $R_F$ (ohm) | $ I_{Load} $ (A) | $ I_F/I_{Load} $ |
|------------------|--------------------|------------------------|--------------|-------------|------------------|------------------|
| 5                | 1.00               | 0.99                   | -0.01        | 0           | 25               | 1.5              |
| 4                | 0.72               | 0.75                   | 0.03         | 0           | 34               | 1.0              |
| 3                | 0.45               | 0.47                   | 0.02         | 0           | 24               | 1.8              |
| 2                | 0.22               | 0.23                   | 0.01         | 0           | 19               | 2.2              |
| 1                | 0.06               | 0.11                   | 0.05         | 0           | 19               | 2.2              |

| Fault location # | Fault dist. (p.u.) | Estimated dist. (p.u.) | Error (p.u.) | $R_F$ (ohm) | $ I_{Load} $ (A) | $ I_F/I_{Load} $ |
|------------------|--------------------|------------------------|--------------|-------------|------------------|------------------|
| 5                | 1.00               | 0.98                   | -0.02        | 500         | 26               | 1.5              |
| 4                | 0.72               | 0.76                   | 0.04         | 500         | 34               | 1.0              |
| 3                | 0.45               | 0.44                   | -0.01        | 500         | 24               | 1.5              |
| 2                | 0.22               | 0.14                   | -0.08        | 500         | 20               | 2.0              |
| 1                | 0.06               | 0.04                   | -0.02        | 500         | 19               | 2.2              |

As shown in the table 1, the results are in line with the simulations.

An interesting, unexpected and earlier undocumented observation was made during the tests: When an earth fault was alternatively conducted through medium voltage (MV) equipment earthing electrode (refer to Fig. 9a), the fault distance measured at the substation was highly affected. A deeper study showed that the earthing impedance of this electrode was in the order of a few hundred ohms and it was not purely resistive, but included a small reactive component. This term affects the fault loop reactance calculation and is an additional error source for the location algorithm.

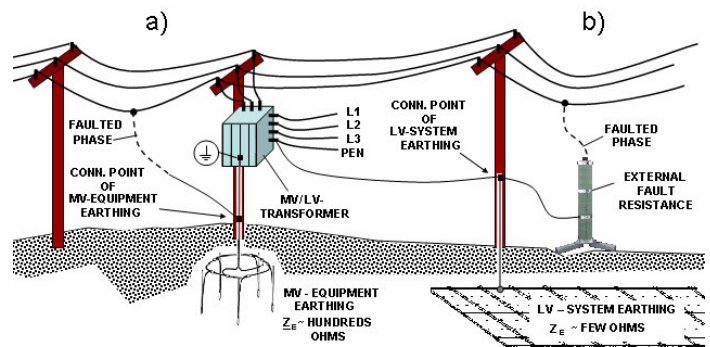


**Figure 9.** Schematic presentation of fault impedance configurations.

**CONCLUSIONS**

The performance of impedance based fault location algorithms has proven to be satisfactory in localizing short-circuit faults, but earth fault localization has remained a challenge in unearthed distribution systems. The main reason why the traditional distance relay type of algorithms cannot be used is the fact that the zero sequence charging current of the feeder is not considered and the assumption that the total load is tapped at the end of the feeder is not correct. The new algorithm introduced in this paper provides a solution to these problems under the conditions that the fault current exceeds the load current and that the fault resistance is purely resistive and not more than a few hundred ohms. However, the first limitation can be avoided, if the “Delta method” is used instead. The behavior of the algorithm was validated through actual field test recordings. Based on these field tests, the fault impedance can in certain cases include a small reactive term, which is an additional error source in the fault distance calculation unless taken into account in the algorithm design.

**REFERENCES**

[1] Hänninen Seppo, 2001, “Single phase earth faults in high impedance grounded networks - Characteristics, indication and location”, VTT Publications 453, 139 p.  
 [2] Hänninen, Seppo & Lehtonen, Matti, 2002, “Earth fault distance computation with fundamental frequency signals based on measurements in substation supply bay”, VTT Research Notes 2153, 40 p.

**MISCELLANEOUS**

**Acknowledgments**

The authors thank the following persons for their support in the performance of the valuable field tests: Markku Viholainen/ABB Oy, Matti Pirskanen/Savon Voima Oyj, Hannu Rautio, Heikki Majanen/Järvi-Suomen Energia Oy, Kari Vastaranta/Sallila Energia Oy and Aimo Rinta-Opas/Koillis-Satakunnan Sähkö Oy.